

Article

Evaluation of Teneligliptin and Retagliptin on the Clearance of Melanosome by Melanophagy in B16F1 Cells

Seong Hyun Kim ¹, Ji-Eun Bae ², Na Yeon Park ¹, Joon Bum Kim ¹, Yong Hwan Kim ¹, So Hyun Kim ¹, Gyeong Seok Oh ¹, Hee Won Wang ¹, Jeong Ho Chang ³  and Dong-Hyung Cho ^{1,4,*}

¹ BK21 FOUR KNU Creative BioResearch Group, School of Life Sciences, Kyungpook National University, Daegu 41566, Republic of Korea; kgj010@naver.com (S.H.K.); yeonie5613@gmail.com (N.Y.P.); kss3213@naver.com (J.B.K.); yoo035913@gmail.com (Y.H.K.); ks90608@naver.com (S.H.K.); dhrujtjr2468@naver.com (G.S.O.)

² KNU LAMP Research Center, Institute of Basic Sciences, Kyungpook National University, Daegu 41566, Republic of Korea; loveg730@naver.com

³ Department of Biology Education, Kyungpook National University, Daegu 41566, Republic of Korea

⁴ Organelle Institute, Kyungpook National University, Daegu 41566, Republic of Korea

* Correspondence: dhcho@knu.ac.kr; Tel.: +82-53-950-5382

Abstract: A specialized membrane-bound organelle, named the melanosome, is central to the storage and transport of melanin as well as melanin synthesis in melanocytes. Although previous studies have linked melanosomal degradation to autophagy, the precise mechanisms remain elusive. Autophagy, a complex catabolic process involving autophagosomes and lysosomes, plays a vital role in cellular constituent degradation. In this study, the role of autophagy in melanosomal degradation was explored, employing a cell-based screening system designed to unveil key pathway regulators. We identified specific dipeptidyl peptidase-4 inhibitors, such as teneligliptin hydrobromide and retagliptin phosphate, as novel agents inducing melanophagy through a comprehensive screening of a ubiquitination-related chemical library. We found that treatment with teneligliptin hydrobromide or retagliptin phosphate not only diminishes melanin content elevated by alpha-melanocyte-stimulating hormone (α -MSH) but also triggers autophagy activation within B16F1 cells. In addition, the targeted inhibition of unc-51-like kinase (ULK1) significantly attenuated both the anti-pigmentation effects and autophagy induced by teneligliptin hydrobromide and retagliptin phosphate in α -MSH-treated cells. Collectively, our data demonstrate a new frontier in understanding melanosomal degradation, identifying teneligliptin hydrobromide and retagliptin phosphate as promising inducers of melanophagy via autophagy activation. This study contributes essential insights into cellular degradation mechanisms and offers potential therapeutic avenues in the regulation of pigmentation.

Keywords: dipeptidyl peptidase-4 inhibitors; teneligliptin hydrobromide; retagliptin phosphate; melanophagy; melanosome



Citation: Kim, S.H.; Bae, J.-E.; Park, N.Y.; Kim, J.B.; Kim, Y.H.; Kim, S.H.; Oh, G.S.; Wang, H.W.; Chang, J.H.; Cho, D.-H. Evaluation of Teneligliptin and Retagliptin on the Clearance of Melanosome by Melanophagy in B16F1 Cells. *Cosmetics* **2024**, *11*, 35. <https://doi.org/10.3390/cosmetics11020035>

Academic Editors: Enzo Berardesca and Bryan Fuller

Received: 26 December 2023

Revised: 19 February 2024

Accepted: 28 February 2024

Published: 1 March 2024



Copyright: © 2024 by the authors. Licensee MDPI, Basel, Switzerland. This article is an open access article distributed under the terms and conditions of the Creative Commons Attribution (CC BY) license (<https://creativecommons.org/licenses/by/4.0/>).

1. Introduction

Autophagy is a conserved and well-regulated cellular degradation process responsible for the recycling of damaged or unnecessary proteins and organelles. In the initiation phase of general autophagy, the activated ULK1 complex, which involves ULK1 and ATG101 along with multiple autophagy-related genes (ATGs), assembles at pre-autophagosome structures (PASs). During the elongation phase, cellular components are engulfed by the phagophore [1,2]. After the formation of the autophagosome is completed, it subsequently combines with the lysosome. It involves the degradation of engulfed cellular components through the action of various enzymes in the lysosomes. Amino acids or peptides, products of autophagy, can be reused by cells [3].

This self-degradative mechanism is crucial for cellular homeostasis maintenance, allowing the selective degradation of specific organelles, proteins, or cellular complexes

through a process known as selective autophagy [4,5]. Specialized receptor proteins often mediate this selectivity through the recognition of unique target degradation signals. In recent years, significant advances have been forged in understanding the mechanisms controlling selective target engulfment in cells. This involves the identification of ubiquitin-mediated selective autophagy receptor proteins, including NBR1, OPTN, NDP52, TAX1BP1, and SQSTM1/p62. These receptors link the target to the autophagosome by interactions with microtubule-associated protein light chain 3 (LC3) or ATG8-family proteins, which is a well-known autophagy-monitoring marker protein [6–10]. LC3-II is produced by the conjugation of cytosolic LC3-I and phosphatidylethanolamine (PE) on the membrane of autophagosomes [1,2]. This requires ATG7, an E1-like enzyme; ATG3, an E2-like enzyme; and the E3-like complex protein, ATG5-ATG12-ATG16L [11]. A vital regulator in the autophagy–lysosomal pathway is transcription factor EB (TFEB) [12]. Through the expression of various key lysosomal genes and autophagy-related genes, TFEB plays a key role in aligning the cellular response to nutrient availability and other stressors, including the mammalian target of rapamycin (mTOR) pathway. This coordination maintains the homeostasis between the cell's anabolic and catabolic processes [13,14].

Skin is a complex organ that functions to maintain homeostasis and defend against environmental factors on the surface of the body. It consists of multiple layers: the epidermis, the dermis, and the subcutaneous layer [15]. The outermost layer of the skin, the epidermis, can be further divided into three layers—the cornified, spinous, and basal layers. The basal layer and granular layer are primarily composed of melanocytes and keratinocytes [16]. Skin color is primarily influenced by melanin, a pigment produced and housed within specialized organelles called melanosomes in melanocytes [17]. Ultraviolet (UV) is a risk factor for various skin disorders. As a protective mechanism against UV, the melanin absorbs UV and is stored, transferred, and generated in melanosomes. Melanosome biogenesis occurs in four different stages [18,19]. In stage I, premelanosomes derive from the trans-Golgi network. And then premelanosome protein (PMEL) fibrils are produced in immature melanosomes. In stage II, melanosomes change in morphology to an ellipsoidal shape due to PMEL fibrils. In stage III, the synthesis of melanin begins. Tyrosinase and related proteins are recruited from tubular elements of early endosomes to vesicles. In stage IV, melanin polymerizes and deposits on the internal fibrils. Finally, mature melanosomes are transferred from the dendritic tip of the melanocytes to keratinocytes. The produced melanin can protect the skin against UV radiation and regulate the pigmentation of skin.

In skin biology, autophagy has emerged as an interesting factor, particularly concerning skin pigmentation and inflammatory responses of the skin [20]. The altered vitiligo melanocytes' responses to stressors have been linked to a reduction in autophagic flux secondary to Nrf2-SQSTM1 pathway dysfunctions. In addition, the autophagy-defective melanocytes exhibited characteristics similar to premature senescence, accompanied by aberrant Nrf2 signaling, redox imbalance, as well as increased lipid oxidation [21]. Melanosomal degradation through melanophagy, a type of selective autophagy, is an essential regulatory mechanism, controlling melanin levels to hinder overproduction or accumulation, which contributes to skin pigmentation balance [22,23]. Recent studies have elucidated that mTOR inhibition, which activates autophagy, reduces melanin synthesis [24]. Various skin-whitening agents such as arbutin, kojic acid, and resveratrol downregulate pigmentation through the mTOR pathway and autophagy [25,26]. In line with this notion, we and other groups also reported that phytochemicals such as hinokitiol, licochalcone A, and ursolic acid exhibit anti-pigmentation effects through enhancing autophagy in melanocytes [22–27]. Underlying players identified in melanophagy included signaling pathways involving α -melanocyte-stimulating hormone (α -MSH), protein kinase A (PKA), and microphthalmia-associated transcription factor (MITF) [28,29]. Depigmentation, a complex process often pursued for cosmetic reasons or specific pigmentation disorders including melasma, albinism, or vitiligo, also interacts with these MITF and PKA mechanisms [17,30].

Most importantly, the relevance of autophagy in skin whitening originates from its ability to regulate melanin content via melanosomal degradation. Recently, we reported that chemicals, including 3,4,5-trimethoxy cinnamate thymol ester (TCTE, also known as melasolv) and nalfuafine hydrochloride, decrease melanin contents by inducing melanophagy in α -MSH-treated B16F1 cells [23,29]. In this study, we further identified teneligliptin hydrobromide and retagliptin phosphate, which are known dipeptidyl peptidase-4 (DPP4) inhibitors, as potent novel melanophagy inducers according to a chemical library screening. In this study, we evaluated the role of teneligliptin hydrobromide and retagliptin phosphate on melanophagy by obstructing a process using the inhibitor of ULK1 in B16F1 cells.

2. Materials and Methods

2.1. Reagents

Teneligliptin hydrobromide (Catalog No. HY-14806A), retagliptin phosphate (Catalog No. HY-112668), and SBI-0206965 (Catalog No. HY-16966) were sourced from MedChem-Express, located in Monmouth Junction, NJ, USA. These compounds were selected for their relevance to our study of cellular processes. Additionally, 3,4,5-trimethoxy cinnamate thymol ester (TCTE), a compound of interest, was synthesized by the Amorepacific Research Group, following a methodology previously described in the literature [31]. This synthesis underscores our commitment to using specialized, research-driven compounds in our experiments. Furthermore, alpha-melanocyte-stimulating hormone (α -MSH, Catalog No. M4135) and bafilomycin A1 (Catalog No. B1793) were procured from Sigma-Aldrich, based in St. Louis, MO, USA. Another key compound, Torin1 (Catalog No. 4247), was obtained from Tocris Bioscience in Bristol, UK. This variety of suppliers highlights our effort to gather the most effective reagents for our research. In terms of genetic materials, we acquired several plasmids from Addgene (Watertown, MA, USA): pEGFP-TFEB (Catalog No. 38119), pmRFPEGFP-LC3 (Catalog No. 21074), and pEGFP-two-pore channel (TPC2) (Catalog No. 80153). These plasmids were instrumental for our cell line studies. Additionally, to generate the pcDNA/TPC2-mRFP-EGFP plasmid, both TPC2 and mRFP-EGFP were amplified with PCR and subcloned into the pcDNA3.1/Myc-His(-)A vector. Lastly, the pEGFP-LC3 plasmid was kindly provided by Tamotsu Yoshimori from Osaka University, Japan. A validated small interfering RNA (siRNA) designed to target mouse Atg5 (sequence: 5'-ACCGGAAACUCAUGGAAUA-3') and scrambled control (sequence: 5'-CCUACGCCACCAUUUCGU-3') were synthesized by Genolution (Seoul, Republic of Korea) [23].

2.2. Cell Culture

B16F1 melanoma cells, a widely used cell line in melanoma research, were obtained from the American Type Culture Collection (ATCC, located in Manassas, VA, USA). These cells were cultured under carefully controlled conditions, specifically in a 5% CO₂ incubator maintained at a temperature of 37 °C. The growth medium used for culturing these cells was Dulbecco's Modified Eagle's Medium (DMEM), with 10% FBS and 1% penicillin/streptomycin, all sourced from Invitrogen, based in Carlsbad, CA, USA. This specific medium composition was chosen to provide optimal growth conditions for the melanoma cells. To create stable cell lines from the B16F1 melanoma cells, the cells were transfected with different plasmids: pEGFP-LC3 to produce B16F1/GFP-LC3 cells, pcDNA3/TPC2-mRFP-EGFP for B16F1/TPC2-mRFP-EGFP cells, and pEGFP-TFEB to create B16F1/GFP-TFEB cells. Transfection was carried out using Lipofectamine 2000, adhering to the protocol provided by the manufacturer (Product No. 11668019, Invitrogen, Carlsbad, CA, USA). Following transfection, the cells underwent a selection process in a medium containing Geneticin at a concentration of 1.25 mg/mL (Product No. 10131035, Invitrogen, Carlsbad, CA, USA). This selection phase lasted for 10 days, during which the cells that successfully integrated the transfected DNA survived and proliferated. Colonies that emerged from single transfected cells were selected to ensure the purity and stability of the cell lines.

To confirm the stability and correct expression of the transfected genes, a fluorescence microscope (Model IX71; Olympus, Tokyo, Japan) was employed.

2.3. Cell Based Library Screening

In our cell-based chemical library screening study, we utilized a specialized ubiquitination compound library from TargetMol (catalog number L8600, located in Boston, MA, USA). This library was chosen for its comprehensive array of compounds that interact with pathways of ubiquitination, a crucial cellular process. The experiment began with the careful seeding of B16/GFP-LC3 cells into a 96-well plate. These cells, known for their GFP-LC3 expression, are ideal for monitoring autophagy. Following seeding, the cells were incubated for 24 h, allowing them to adhere properly and reach a suitable state for treatment. Post incubation, we introduced varied concentrations of the ubiquitination compounds into the wells. This variation in concentration was key to observing a range of cellular responses. The primary assessment method was fluorescence microscopy, focusing on the GFP-LC3 puncta within the cells. The presence and abundance of these puncta indicate autophagic activity, influenced by ubiquitination. To validate our findings, we conducted two separate experiments under identical conditions, both yielding the results.

2.4. Assay for Melanin Content

To measure melanin content, we adapted a method previously described in the literature [32]. The experiment began with B16F1 cells, which were first pretreated with α -MSH for a duration of 36 h. This initial step was crucial for stimulating melanin production. After this pretreatment, the cells were then incubated with various concentrations of teneligliptin hydrobromide (10 and 100 μ M), retagliptin phosphate (10 and 100 μ M), or TCTE at a concentration of 10 μ g/mL for 24 h. These specific compounds and concentrations were chosen to assess their impact on melanin synthesis. Following the incubation period, the cells underwent trypsinization. This process detached the cells from their growth surface, allowing for the formation of a cell pellet. The cell pellet was then dissolved in a specialized solubilization buffer, consisting of 1N NaOH with a 10% DMSO solution. This buffer was used to effectively lyse the cells and release the melanin content. The mixture containing the dissolved cells was then heated at 100 °C for 30 min. This heating step was critical to ensure complete cell lysis and release of all melanin. The relative melanin amounts in the solution were subsequently measured by calculating the absorbance at 405 nm. This measurement was carried out using a microplate reader from BioTek (Santa Clara, CA, USA).

2.5. Autophagy Analysis

To analyze the nuclear translocation of transcription factor EB (TFEB), B16F1/GFP-TFEB cells underwent treatment with various compounds. Specifically, these cells were treated with Torin1 at a concentration of 0.25 μ M for a duration of 1 h. Additionally, they were exposed to either teneligliptin hydrobromide (100 μ M) or retagliptin phosphate (100 μ M) for an extended period of 24 h. Post treatment, cells exhibiting nuclear localization of TFEB were identified and quantitatively analyzed using a fluorescence microscope. This process enabled the precise measurement of TFEB translocation into the nucleus. B16F1/GFP-LC3 cells were pre-incubated with α -MSH for a period of 36 h. Following this pre-treatment, these cells were then incubated with one of the following agents: teneligliptin hydrobromide (100 μ M), retagliptin phosphate (100 μ M), or TCTE at a concentration of 10 μ g/mL. This step was carried out for a duration of 24 h. The primary objective of this experiment was to determine the extent of autophagy within the cells. This determination was based on the observation of GFP-LC3 punctate structures, indicative of autophagosomes, using a high-resolution confocal microscope (LSM 800, Carl Zeiss, Thornwood, NY, USA). The percentage of cells displaying these GFP-LC3 puncta was carefully recorded and analyzed.

2.6. Melanophagy Assay

For the melanophagy analysis, B16F1/TPC2-mRFP-EGFP cells were meticulously prepared on coverslips placed in culture well plates to facilitate detailed observation. These cells underwent an initial pre-treatment phase with α -MSH at a concentration of 0.5 μ M for a duration of 12 h. This phase was followed by a further incubation period, during which the cells were either exposed to SBI-0206965 at a concentration of 5 μ M or left untreated for an additional 24 h. Concurrently, these cells were also subjected to treatment with either teneligliptin hydrobromide (100 μ M) or retagliptin phosphate (100 μ M) for the same 24 h period. Post treatment, the cells underwent a meticulous cleaning process using PBS (pH 7.4), ensuring the removal of any residual reagents. This was followed by fixation of the cells with a 4% paraformaldehyde solution and maintenance at room temperature for a period of 20 min. Subsequent to this fixation process, the cells were again washed thoroughly with PBS to remove any traces of paraformaldehyde. Once prepared, the cells were mounted on the previously prepared coverslips. These mounted samples were then scrutinized under a high-precision confocal microscope (LSM 800).

2.7. Western Blotting

For the preparation of lysates from all samples, a 2 \times Laemmli sample buffer was employed. This buffer comprised a specific composition of Tris buffer (62.5 mM Tris-HCl, pH 6.8, β -mercaptoethanol, and 0.01%, 25% glycerol, 2% SDS, 5% bromophenol blue (#161073, Bio-Rad Laboratories, Hercules, CA, USA)). Following this, the total protein content in each sample was quantitatively determined utilizing the Bradford assay, using the kit #5000006, also provided by Bio-Rad. After establishing the protein concentration, the samples were then subjected to a separation process via 12% SDS-PAGE. Post separation, the proteins were carefully transferred onto PVDF membranes. For the detection of specific proteins, these membranes were incubated with a set of primary antibodies. This set included anti-LC3 at a dilution of 1:2000 (# NB100-2220), anti-ATG5 at a dilution of 1:3000 (# NB110-53818), and anti-ACTA1 at a dilution of 1:10000 (product code NB60-501; both antibodies procured from NOVUS Biologicals, Littleton, CO, USA). To facilitate the detection of these protein levels, the membranes were further incubated with horseradish peroxidase (HRP)-conjugated secondary antibodies, obtained from Pierce (Rockford, IL, USA). The protein levels in each sample were then meticulously analyzed using CS analyzer software 4, provided by ATTO (Tokyo, Japan). Additionally, for enhanced protein detection, the membranes were again incubated with horseradish peroxidase (HRP)-conjugated secondary antibodies (#7074 and #7076, from Cell Signaling Technology, Danvers, MA, USA). The generation of a chemiluminescent signal was achieved by employing the Clarity Western ECL substrate (product code W3680-010, Bio-Rad). Subsequently, densitometry analysis was conducted on the immunoblots. These immunoblots were scanned using an AE-9300 Ez-Capture MG Hours Image Saver HR image capture tool (model WSE-7120L, ATTO, Tokyo, Japan). The expression levels of each protein were normalized against the levels of ACTA1, ensuring an accurate comparative analysis.

2.8. Statistical Analysis

To acquire data, more than three independent experiments were conducted and the results are indicated as the mean \pm SEM. Graph data analysis was addressed using GraphPad Prism 8 (GraphPad Software, San Diego, CA, USA). One-way analysis of variance (ANOVA) was used for the statistical evaluation, with significance levels set at * $p < 0.05$, ** $p < 0.01$, and *** $p < 0.001$.

3. Results

3.1. Teneligliptin Hydrobromide and Retagliptin Phosphate Activate Autophagy in B16F1 Cells

Melanophagy, melanosomal selective autophagy, serves as a crucial mechanism for maintaining melanosome homeostasis. In our pursuit for identifying novel regulators of melanophagy, we established a high-content screening system utilizing B16F1 cells stably

over-expressing EGFP-fused light chain 3 (B16F1/EGFP-LC3). We screened a chemical library comprising ubiquitination-related small chemical inhibitors and identified several putative candidates, including teneligliptin hydrobromide and retagliptin phosphate, both recognized as specific dipeptidyl peptisase-4 (DPP4) inhibitors. To validate these results, we investigated the effects of teneligliptin hydrobromide and retagliptin phosphate on autophagy in B16F1/GFP-LC3 cells. As depicted in Figure 1A, the level of immunoreactive LC3 significantly increased in cells treated with either compound. 3,4,5-trimethoxy cinnamate thymol ester (TCTE) was used as a positive control for melanophagy [23].

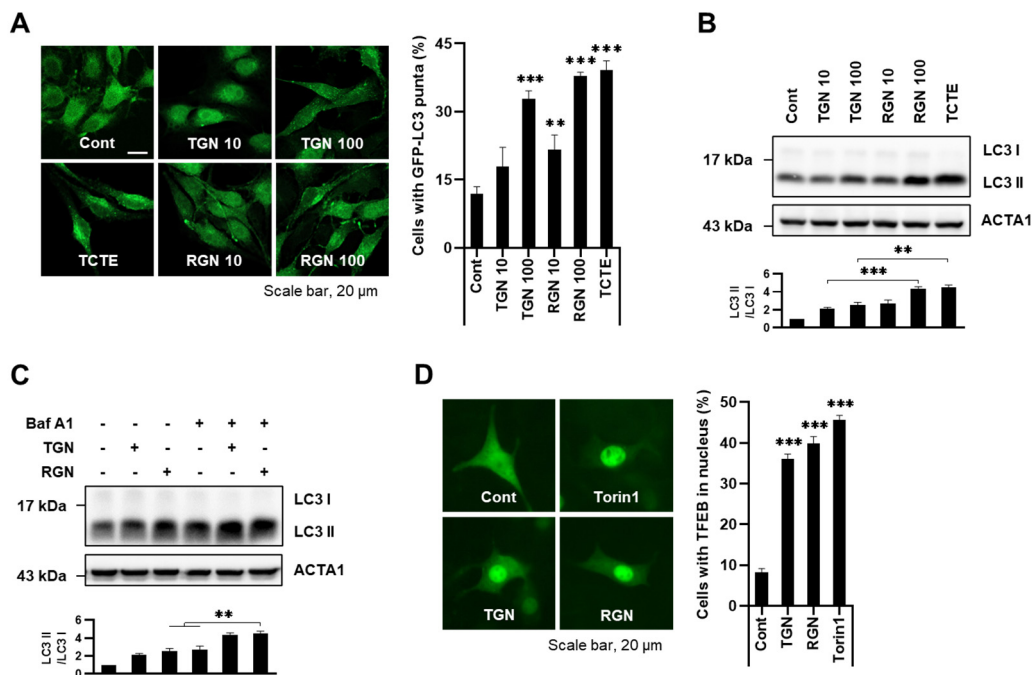


Figure 1. Teneligliptin hydrobromide and retagliptin phosphate induce autophagy through TFEB translocation: (A,B) B16F1/GFP-LC3 cells were treated with either teneligliptin hydrobromide (TGN, 10, 100 μ M), retagliptin phosphate (RGN, 10, 100 μ M), or 3,4,5-trimethoxy cinnamate thymol ester (TCTE, 10 μ g/mL). (A) Then, 24 h later, the treated cells were fixed to be imaged for green fluorescence. Cells in which autophagy was induced were analyzed by counting GFP-LC3 punctate dots under a confocal microscope. (B) The protein expression of LC3 was then examined by Western blotting. (C) B16F1 cells were treated with teneligliptin hydrobromide (TGN, 100 μ M) or retagliptin phosphate (RGN, 100 μ M), with or without bafilomycin A1 (Baf A1, 100 nM), for 6 h. The LC3 level was then examined by Western blotting. (D) B16F1/GFP-TFEB cells were exposed to teneligliptin hydrobromide (TGN, 100 μ M) or retagliptin phosphate (RGN, 100 μ M) for 24 h or Torin1 (0.25 μ M) for 1 h. The cells were fixed for fluorescence imaging, and the nuclear translocation of TFEB was assessed. The scale bar indicates 20 μ m. (n = 3, ** $p < 0.01$ and *** $p < 0.001$).

During the formation of autophagosomes, cytosolic LC3 I conjugates with phosphatidylethanolamine (PE) and then LC3 I is converted to LC3 II on the surface of autophagosomes [1,2]. The conversion of LC3 protein (LC3 I to LC3 II) is a commonly accepted measure of autophagy activation. Treatment with teneligliptin hydrobromide or retagliptin phosphate revealed enhanced LC3 II levels in cells (Figure 1B). Furthermore, we assessed autophagic flux, the complete autophagy process, based on the formation of autophagosomes from degradation. B16F1 cells were incubated with teneligliptin or retagliptin in the presence or absence of the lysosome fusion inhibitor bafilomycin A1. It led to even greater increases in LC3 II level, suggesting that teneligliptin hydrobromide or retagliptin phosphate augments autophagy flux in B16F1 cells (Figure 1C).

To confirm the effect of teneligliptin hydrobromide and retagliptin phosphate on autophagy induction, we observed transcription factor EB (TFEB) locations using B16F1/GFP-

TFEB cells. In response to autophagy stimuli, TFEB translocates from the cytosol to the nucleus to activate autophagy-associated target genes, including various autophagy-related genes (ATGs) [12]. Consistently, treatment with teneligliptin hydrobromide or retagliptin phosphate led to the nuclear translocation of TFEB, akin to the effect induced by Torin1, a potent mammalian target of rapamycin (mTOR) inhibitor (Figure 1D). In summary, these findings suggest that teneligliptin hydrobromide or retagliptin phosphate activates autophagy in B16F1 cells.

3.2. Teneligliptin Hydrobromide and Retagliptin Phosphate Inhibit α -MSH-Stimulated Melanogenesis in B16F1 Cells

We then further addressed the effect of teneligliptin hydrobromide or retagliptin phosphate effect on melanophagy by exploring the melanin content regulation. A cell viability assay showed that these compounds were not cytotoxic at a high concentration (100 μ M) (Figure 2A). To assess the whitening effect, B16F1 cells stimulated with alpha-melanocyte-stimulating hormone (α -MSH) were treated with either teneligliptin hydrobromide or retagliptin phosphate and melanin content was analyzed. When skin is exposed to ultraviolet (UV), α -MSH is released, and then melanin synthesis begins in melanocytes [29]. Despite the treatment with α -MSH, teneligliptin hydrobromide or retagliptin phosphate significantly inhibited melanogenesis in B16F1 cells (Figure 2B,C).

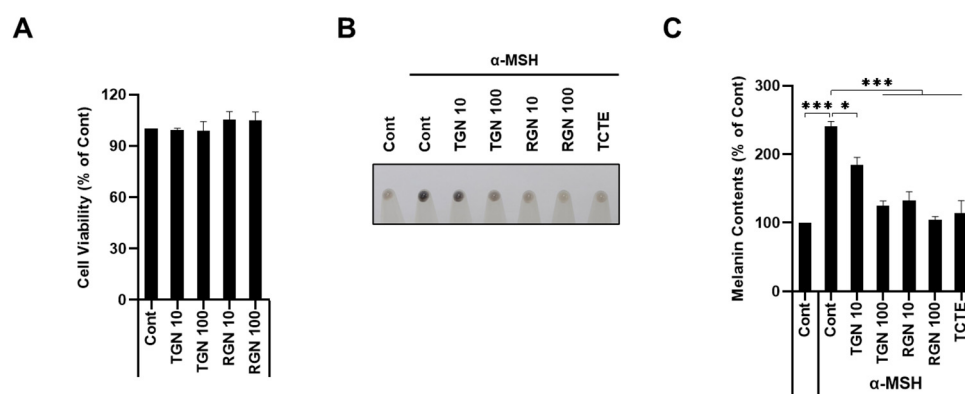


Figure 2. Teneligliptin hydrobromide and retagliptin phosphate induce anti-pigmentation in B16F1 cells treated with α -MSH: (A) B16F1 cells were treated with teneligliptin hydrobromide (TGN, 10, 100 μ M) or retagliptin phosphate (RGN, 10, 100 μ M) for 24 h, then cell viability was determined by CCK-8 assay. (B) B16F1 cells were pre-treated with alpha-melanocyte-stimulating hormone (α -MSH, 0.5 μ M) for 36 h and then additionally exposed to teneligliptin hydrobromide (TGN, 10, 100 μ M), retagliptin phosphate (RGN, 10, 100 μ M) or 3,4,5-trimethoxy cinnamate thymol ester (TCTE, 10 μ g/mL) for 24 h. (B) Melanin content is shown in cell pellets. (C) The melanin content was measured by assessing absorbance at 405 nm through a microplate reader, as outlined in the Materials and Methods Section. (n = 3, * p < 0.05 and *** p < 0.001).

3.3. Teneligliptin Hydrobromide and Retagliptin Phosphate Promote Melanophagy in B16F1 Cells

To investigate melanophagy induction, we generated a melanophagy-addressing system, TPC2-mRFP-EGFP. The tandem assay principle relies on the differing pH stability of red (mRFP) and green (EGFP) fluorescent proteins. In the activation of melanophagy, autophagosomes engulf targeted melanosomes and deliver to the lysosomes. And then melanosomes are degraded in autolysosomes. In the inside of lysosomes, the acid-sensitive EGFP signal is easily quenched, whereas the more stable mRFP signal persists, serving as an indicator of a melanophagic process. Using this system, B16F1/TPC2-mRFP-EGFP cells pre-exposed to α -MSH were further treated with teneligliptin hydrobromide or retagliptin phosphate. Treatment with teneligliptin and retagliptin increased RFP-positive signals, as demonstrated in Figure 3A,B. Furthermore, not only treatment with bafilomycin A1 but also the depletion of Atg5 by RNA interference reversed the increased RFP-positive signals by either teneligliptin hydrobromide or retagliptin phosphate (Figure 3A,B). These

results indicate that both teneligliptin hydrobromide and retagliptin phosphate activate melanophagy in B16F1 cells.

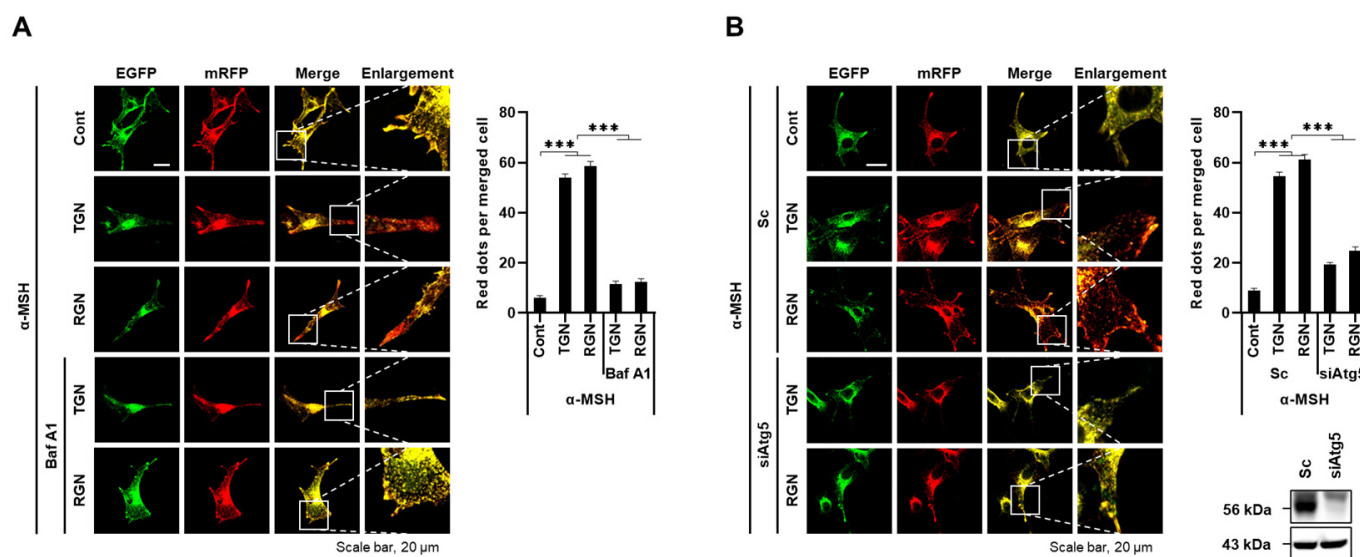


Figure 3. Teneligliptin hydrobromide and retagliptin phosphate induce melanosomal degradation via autophagy: (A) First, 0.5 μM $\alpha\text{-MSH}$ -treated B16F1/TPC2-mRFP-EGFP cells were exposed to teneligliptin hydrobromide (TGN, 100 μM) or retagliptin phosphate (RGN, 100 μM) for 18 h, with or without 100nM bafilomycin (Baf A1) for 6 h. After fixation, the distribution of TPC2-mRFP-EGFP in the cells was imaged with confocal microscopy. (B) B16F1/TPC2-mRFP-EGFP cells were transfected with non-specific control siRNA (Sc) or siRNA targeting Atg5 (siAtg5). After 24 h transfection, the cells were further treated with 0.5 μM $\alpha\text{-MSH}$ for 36 h and then incubated with teneligliptin hydrobromide (TGN, 100 μM) or retagliptin phosphate (RGN, 100 μM). The number of RFP-only signals per cells was analyzed with merged images. The protein expression of Atg5 was then assessed by Western blotting. $n = 3$ and $*** p < 0.001$.

3.4. ULK1 Inhibitor Decreases Melanophagy Induced by Teneligliptin Hydrobromide and Retagliptin Phosphate

We then explored the effects of autophagy inhibition on teneligliptin hydrobromide- or retagliptin phosphate-induced melanophagy. As previously shown, the activation of autophagy led to a decline in melanin content. unc-51-like kinase (ULK1), a key regulatory molecule in autophagy activation, is consistent with our hypothesis. SBI-0206965 is recognized for its role as an autophagy inhibitor, exerting selective inhibition of ULK1 phosphorylation [33]. The inhibition of ULK1 by SBI-0206965 strongly suppressed either teneligliptin hydrobromide- or retagliptin phosphate-mediated depigmentation in $\alpha\text{-MSH}$ -stimulated B16F1 cells (Figure 4A,B).

Additionally, we validated that teneligliptin hydrobromide- or retagliptin phosphate-induced autophagy is ULK1-dependent. SBI-0206965 suppressed the teneligliptin hydrobromide- or retagliptin phosphate-induced conversion of LC3 I to LC3 II (Figure 5A). Moreover, the ULK1 inhibitor induces the RFP-positive signal blockade increased by teneligliptin hydrobromide or retagliptin phosphate treatment (Figure 5B). Taken together, these results suggest that either teneligliptin hydrobromide or retagliptin phosphate induces melanosomal degradation via the ULK-dependent autophagy pathway.

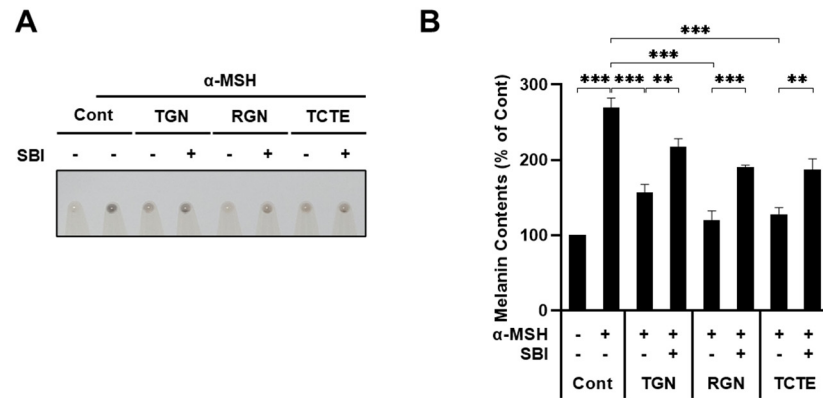


Figure 4. Inhibition of autophagy reverses the whitening effects of teneligliptin hydrobromide and retagliptin phosphate: (A,B) B16F1 cells were pre-treated with 0.5 μM $\alpha\text{-MSH}$ for 12 h and then the cells were incubated in the presence or absence of SBI-0206965 (SBI, 5 μM) for 24 h and additionally exposed to teneligliptin hydrobromide (TGN, 100 μM) or retagliptin phosphate (RGN, 100 μM) for 24 h. (A) Melanin content is shown in cell pellets. (B) Content in the cells was quantified by addressing absorbance at 405 nm using a microplate reader, as detailed in the Materials and Methods Section. (n = 3 and ** $p < 0.01$, *** $p < 0.001$).

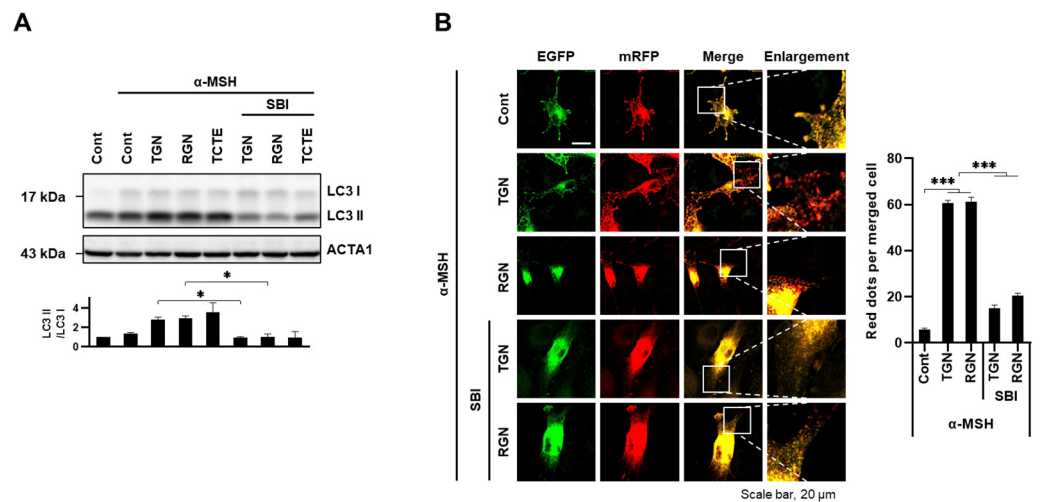


Figure 5. Inhibition of autophagy decreases melanosomal degradation by teneligliptin hydrobromide and retagliptin phosphate: (A,B) B16F1 cells or B16F1/TPC2-mRFP-EGFP cells were pre-treated with 0.5 μM $\alpha\text{-MSH}$ for 12 h. And the cells were further incubated with or without SBI-0206965 (SBI, 5 μM) for 24 h and additionally exposed to teneligliptin hydrobromide (TGN, 100 μM) or retagliptin phosphate (RGN, 100 μM) for an additional 24 h. (A) The protein expression of LC3 was then examined by Western blotting. (B) After fixation, the distribution of TPC2-mRFP-EGFP was imaged under a confocal microscope. The number of RFP-positive signal dots per cells was quantified from the merged cell images. The scale bar indicates 20 μm . (n = 3, * $p < 0.05$, *** $p < 0.001$).

4. Discussion

The primary controlling factor for mammalian skin pigmentation is melanin content. Consequently, abnormalities in the homeostasis of melanin synthesis and its transportation to keratinocytes lead to various pigmentary disorders, including vitiligo, ash leaf spots, as well as melasma [34–36]. While the regulation of melanosome quality and quantity through melanophagy is essential for understanding these pigmentary diseases, the underlying mechanisms governing melanophagy remain elusive. Recent advances have demonstrated that ubiquitination plays a pivotal role in the specific cargo degradation of intracellular components through selective autophagy. Fundamentally, ubiquitination functions as a marker, guiding defective or targeted organelles for clearance via autophagy. In our

research, we analyzed a ubiquitination compound library and identified several potential autophagy inducers, including dBET1 as well as the dipeptidyl peptidase-4 (DPP4) inhibitors teneligliptin hydrobromide and retagliptin phosphate. Remarkably, previous studies have shown that dBET1, which inhibits BRD family proteins, also activates autophagy in diverse cell types [37].

Previously, it has been reported that DPP4 inhibitors, commonly used as antidiabetic agents, exert anti-inflammatory and antioxidant effects [38,39]. Recent evidence indicated that DPP4 inhibitors can enhance autophagic flux, potentially offering cellular stress protection [39]. However, the exact mechanisms of how DPP4 inhibitors modulate autophagy remain unexplored. Notably, Song et al. recently revealed that another DPP4 inhibitor, gemigliptin, activates autophagy to ameliorate non-alcoholic steatohepatitis (NASH) in cell and mouse models [40]. Gemigliptin alleviated inflammasome activation via unc-51-like kinase (ULK1)-dependent autophagy induction and reduced lipid accumulation, inflammation, and fibrosis in NASH models [40]. On the other hand, Kong et al. demonstrated that the inhibition of DPP4 by sitagliptin reduces excessive autophagy via p62-Keap1-Nrf2 signaling to attenuate ROS stress in acute injury models of the lungs [39]. Arab et al. demonstrated that sitagliptin induces autophagy through the inhibition of mTOR, a finding that aligns with Figure 1D [41]. In our study, we also observed that the DPP4 inhibitors trigger autophagy by regulating mTOR signaling. Thus, further evaluation of the pathways related to autophagy involving mTOR signaling will enhance our understanding of how melanosome degradation occurs in cells treated with teneligliptin hydrobromide and retagliptin phosphate, contributing to a deeper insight into the underlying mechanisms.

DPP4 is highly expressed in normal melanocytes; however, its expression is reduced when melanocytes are transformed into melanoma [42,43], suggesting that DPP4 suppresses the malignant phenotype. Nonetheless, the exact role of DPP4 in skin pigmentation remains unclear. In this study, we found that the DPP4 inhibitors teneligliptin hydrobromide and retagliptin phosphate highly reduce melanin contents by promoting the degradation of melanosomes in alpha-melanocyte-stimulating hormone (α -MSH)-stimulated B16F1 cells (Figures 2 and 3), which was restored by inhibition of ULK1 (Figure 4). Thus, our findings suggest that the inhibition of DPP4 induces autophagy in a ULK1-dependent manner [40]. Previous studies have shown that DPP4 inhibitors play a critical role in reducing cellular reactive oxygen species (ROS) levels and the production of various cytokines, which modulate immune responses [44]. The NF- κ B signaling pathway is well documented for its central role in inflammatory response regulation [45]. Activation of NF- κ B has been linked to increased melanogenesis, particularly in post-inflammatory conditions. Elevated NF- κ B levels can amplify melanocyte activity, leading to increased melanin production [46]. Consequently, hyperpigmentation can occur in skin regions where NF- κ B has been excessively activated secondary to inflammation [46,47]. Additionally, DPP4 inhibitors appear to modulate autophagy, which also regulates NF- κ B activation by degrading its components, thereby potentially limiting its pro-inflammatory effects [48]. Therefore, the combined effects of DPP4 inhibitors on both NF- κ B and autophagy suggest their potential role in conditions marked by inflammation and melanogenesis.

In skin aging, the activity of autophagy declines due to various stresses, including repeated exposure to UV and ROS [49]. Hence, restoring this process could improve the condition of aged dermal fibroblasts, keratinocytes, and melanocytes [49,50]. Since our study focused on B16F1 mouse melanoma cells, evaluating the effect of teneligliptin hydrobromide and retagliptin phosphate on melanophagy in other skin models such as human primary melanocytes and organoids could reveal the potential of these compounds as cosmetic agents for treating aged skin and pigmentary disorders.

In conclusion, DPP4 inhibitors, beyond their established roles in glucose regulation and inflammation, play a notable role in modulating melanogenesis via their effects on autophagy. Our findings underscore the potential of these inhibitors as cosmetic agents for pigmentary disorders and conditions influenced by melanin production.

Author Contributions: S.H.K. (Seong Hyun Kim): conceptualization, investigation, data curation, writing—original draft; J.-E.B.: conceptualization, investigation, data curation; N.Y.P.: investigation; J.B.K.: investigation; Y.H.K.: investigation; S.H.K. (So Hyun Kim): investigation; G.S.O.: investigation; H.W.W.: investigation; J.H.C.: conceptualization; D.-H.C.: supervision, writing—review and editing, funding acquisition. All authors have read and agreed to the published version of the manuscript.

Funding: This research was supported by the National Research Foundation of Korea, and funded by the Ministry of Science & ICT [2020R1A2C2003523] and by the Korea Institute for Advancement of Technology funded by the Ministry of Trade, Industry and Energy [P0025489]. This research was also supported by the ORGASIS corporation.

Institutional Review Board Statement: Not applicable.

Informed Consent Statement: Not applicable.

Data Availability Statement: All data are available in the article.

Conflicts of Interest: The authors declare no conflicts of interest.

References

1. Ohsumi, Y. Molecular dissection of autophagy: Two ubiquitin-like systems. *Nat. Rev. Mol. Cell Biol.* **2001**, *2*, 211–216. [[CrossRef](#)]
2. Geng, J.; Klionsky, D.J. The Atg8 and Atg12 ubiquitin-like conjugation systems in macroautophagy. ‘Protein modifications: Beyond the usual suspects’ review series. *EMBO Rep.* **2008**, *9*, 859–864. [[CrossRef](#)]
3. Li, X.; He, S.; Ma, B. Autophagy and autophagy-related proteins in cancer. *Mol. Cancer* **2020**, *19*, 12. [[CrossRef](#)]
4. Li, W.; He, P.; Huang, Y.; Li, Y.F.; Lu, J.; Li, M.; Kurihara, H.; Luo, Z.; Meng, T.; Onishi, M.; et al. Selective autophagy of intracellular organelles: Recent research advances. *Theranostics* **2021**, *11*, 222–256. [[CrossRef](#)]
5. Vargas, J.N.S.; Hamasaki, M.; Kawabata, T.; Youle, R.J.; Yoshimori, T. The mechanisms and roles of selective autophagy in mammals. *Nat. Rev. Mol. Cell Biol.* **2023**, *24*, 167–185. [[CrossRef](#)]
6. Pankiv, S.; Clausen, T.H.; Lamark, T.; Brech, A.; Bruun, J.A.; Outzen, H.; Overvatn, A.; Bjorkoy, G.; Johansen, T. p62/SQSTM1 binds directly to Atg8/LC3 to facilitate degradation of ubiquitinated protein aggregates by autophagy. *J. Biol. Chem.* **2007**, *282*, 24131–24145. [[CrossRef](#)]
7. Kirkin, V.; Lamark, T.; Johansen, T.; Dikic, I. NBR1 cooperates with p62 in selective autophagy of ubiquitinated targets. *Autophagy* **2009**, *5*, 732–733. [[CrossRef](#)]
8. Shen, W.C.; Li, H.Y.; Chen, G.C.; Chern, Y.; Tu, P.H. Mutations in the ubiquitin-binding domain of OPTN/optineurin interfere with autophagy-mediated degradation of misfolded proteins by a dominant-negative mechanism. *Autophagy* **2015**, *11*, 685–700. [[CrossRef](#)] [[PubMed](#)]
9. von Muhlinen, N.; Thurston, T.; Ryzhakov, G.; Bloor, S.; Randow, F. NDP52, a novel autophagy receptor for ubiquitin-decorated cytosolic bacteria. *Autophagy* **2010**, *6*, 288–289. [[CrossRef](#)] [[PubMed](#)]
10. Sarraf, S.A.; Shah, H.V.; Kanfer, G.; Pickrell, A.M.; Holtzclaw, L.A.; Ward, M.E.; Youle, R.J. Loss of TAX1BP1-Directed Autophagy Results in Protein Aggregate Accumulation in the Brain. *Mol. Cell* **2020**, *80*, 779–795.e710. [[CrossRef](#)] [[PubMed](#)]
11. Liu, C.; Ji, L.; Hu, J.; Zhao, Y.; Johnston, L.J.; Zhang, X.; Ma, X. Functional Amino Acids and Autophagy: Diverse Signal Transduction and Application. *Int. J. Mol. Sci.* **2021**, *22*, 11427. [[CrossRef](#)] [[PubMed](#)]
12. Settembre, C.; Di Malta, C.; Polito, V.A.; Garcia Arencibia, M.; Vetrini, F.; Erdin, S.; Erdin, S.U.; Huynh, T.; Medina, D.; Colella, P.; et al. TFEB links autophagy to lysosomal biogenesis. *Science* **2011**, *332*, 1429–1433. [[CrossRef](#)]
13. Napolitano, G.; Ballabio, A. TFEB at a glance. *J. Cell Sci.* **2016**, *129*, 2475–2481. [[CrossRef](#)] [[PubMed](#)]
14. Vega-Rubin-de-Celis, S.; Pena-Llopis, S.; Konda, M.; Brugarolas, J. Multistep regulation of TFEB by MTORC1. *Autophagy* **2017**, *13*, 464–472. [[CrossRef](#)]
15. Hofmann, E.; Schwarz, A.; Fink, J.; Kamolz, L.P.; Kotzbeck, P. Modelling the Complexity of Human Skin In Vitro. *Biomedicines* **2023**, *11*, 794. [[CrossRef](#)]
16. D’Mello, S.A.; Finlay, G.J.; Baguley, B.C.; Askarian-Amiri, M.E. Signaling Pathways in Melanogenesis. *Int. J. Mol. Sci.* **2016**, *17*, 1144. [[CrossRef](#)]
17. Le, L.; Sires-Campos, J.; Raposo, G.; Delevoye, C.; Marks, M.S. Melanosome Biogenesis in the Pigmentation of Mammalian Skin. *Integr. Comp. Biol.* **2021**, *61*, 1517–1545. [[CrossRef](#)]
18. Bissig, C.; Rochin, L.; van Niel, G. PMEL Amyloid Fibril Formation: The Bright Steps of Pigmentation. *Int. J. Mol. Sci.* **2016**, *17*, 1438. [[CrossRef](#)] [[PubMed](#)]
19. Hida, T.; Kamiya, T.; Kawakami, A.; Ogino, J.; Sohma, H.; Uhara, H.; Jimbow, K. Elucidation of Melanogenesis Cascade for Identifying Pathophysiology and Therapeutic Approach of Pigmentary Disorders and Melanoma. *Int. J. Mol. Sci.* **2020**, *21*, 6129. [[CrossRef](#)]
20. Kovacs, D.; Cardinali, G.; Picardo, M.; Bastonini, E. Shining Light on Autophagy in Skin Pigmentation and Pigmentary Disorders. *Cells* **2022**, *11*, 2999. [[CrossRef](#)]

21. Zhang, C.F.; Gruber, F.; Ni, C.; Mildner, M.; Koenig, U.; Karner, S.; Barresi, C.; Rossiter, H.; Narzt, M.S.; Nagelreiter, I.M.; et al. Suppression of autophagy dysregulates the antioxidant response and causes premature senescence of melanocytes. *J. Investig. Dermatol.* **2015**, *135*, 1348–1357. [[CrossRef](#)]
22. Park, H.J.; Jo, D.S.; Choi, D.S.; Bae, J.E.; Park, N.Y.; Kim, J.B.; Chang, J.H.; Shin, J.J.; Cho, D.H. Ursolic acid inhibits pigmentation by increasing melanosomal autophagy in B16F1 cells. *Biochem. Biophys. Res. Commun.* **2020**, *531*, 209–214. [[CrossRef](#)]
23. Park, H.J.; Jo, D.S.; Choi, H.; Bae, J.E.; Park, N.Y.; Kim, J.B.; Choi, J.Y.; Kim, Y.H.; Oh, G.S.; Chang, J.H.; et al. Melasolv induces melanosome autophagy to inhibit pigmentation in B16F1 cells. *PLoS ONE* **2020**, *15*, e0239019. [[CrossRef](#)]
24. Tsao, Y.T.; Huang, Y.F.; Kuo, C.Y.; Lin, Y.C.; Chiang, W.C.; Wang, W.K.; Hsu, C.W.; Lee, C.H. Hinokitiol Inhibits Melanogenesis via AKT/mTOR Signaling in B16F10 Mouse Melanoma Cells. *Int. J. Mol. Sci.* **2016**, *17*, 248. [[CrossRef](#)] [[PubMed](#)]
25. Kim, E.S.; Jo, Y.K.; Park, S.J.; Chang, H.; Shin, J.H.; Choi, E.S.; Kim, J.B.; Seok, S.H.; Kim, J.S.; Oh, J.S.; et al. ARP101 inhibits alpha-MSH-stimulated melanogenesis by regulation of autophagy in melanocytes. *FEBS Lett.* **2013**, *587*, 3955–3960. [[CrossRef](#)] [[PubMed](#)]
26. Zou, N.; Wei, Y.; Li, F.; Yang, Y.; Cheng, X.; Wang, C. The inhibitory effects of compound Muniziqi granule against B16 cells and harmine induced autophagy and apoptosis by inhibiting Akt/mTOR pathway. *BMC Complement. Altern. Med.* **2017**, *17*, 517. [[CrossRef](#)]
27. Zhang, Y.; Gao, M.; Chen, L.; Zhou, L.; Bian, S.; Lv, Y. Licochalcone A restrains microphthalmia-associated transcription factor expression and growth by activating autophagy in melanoma cells via miR-142-3p/Rheb/mTOR pathway. *Phytother. Res.* **2020**, *34*, 349–358. [[CrossRef](#)]
28. Yoon, J.H.; Youn, K.; Jun, M. Discovery of Pinostrobin as a Melanogenic Agent in cAMP/PKA and p38 MAPK Signaling Pathway. *Nutrients* **2022**, *14*, 3713. [[CrossRef](#)]
29. Lee, H.J.; Kim, S.H.; Kim, Y.H.; Kim, S.H.; Oh, G.S.; Bae, J.E.; Kim, J.B.; Park, N.Y.; Park, K.; Yeom, E.; et al. Nalfurafine Hydrochloride, a kappa-Opioid Receptor Agonist, Induces Melanophagy via PKA Inhibition in B16F1 Cells. *Cells* **2022**, *12*, 146. [[CrossRef](#)]
30. Bento-Lopes, L.; Cabaco, L.C.; Charneca, J.; Neto, M.V.; Seabra, M.C.; Barral, D.C. Melanin's Journey from Melanocytes to Keratinocytes: Uncovering the Molecular Mechanisms of Melanin Transfer and Processing. *Int. J. Mol. Sci.* **2023**, *24*, 11289. [[CrossRef](#)]
31. Kang, H.H.; Rho, H.S.; Hwang, J.S.; Oh, S.G. Depigmenting activity and low cytotoxicity of alkoxy benzoates or alkoxy cinnamate in cultured melanocytes. *Chem. Pharm. Bull.* **2003**, *51*, 1085–1088. [[CrossRef](#)] [[PubMed](#)]
32. Tsuboi, T.; Kondoh, H.; Hiratsuka, J.; Mishima, Y. Enhanced melanogenesis induced by tyrosinase gene-transfer increases boron-uptake and killing effect of boron neutron capture therapy for amelanotic melanoma. *Pigment. Cell Res.* **1998**, *11*, 275–282. [[CrossRef](#)] [[PubMed](#)]
33. Egan, D.F.; Chun, M.G.; Vamos, M.; Zou, H.; Rong, J.; Miller, C.J.; Lou, H.J.; Raveendra-Panickar, D.; Yang, C.C.; Sheffler, D.J.; et al. Small Molecule Inhibition of the Autophagy Kinase ULK1 and Identification of ULK1 Substrates. *Mol. Cell* **2015**, *59*, 285–297. [[CrossRef](#)] [[PubMed](#)]
34. Lee, B.W.; Schwartz, R.A.; Janniger, C.K. Melasma. *G. Ital. Dermatol. Venereol.* **2017**, *152*, 36–45. [[CrossRef](#)]
35. Bellei, B.; Pitisci, A.; Ottaviani, M.; Ludovici, M.; Cota, C.; Luzi, F.; Dell'Anna, M.L.; Picardo, M. Vitiligo: A possible model of degenerative diseases. *PLoS ONE* **2013**, *8*, e59782. [[CrossRef](#)]
36. Gutman, I.; Dunn, D.; Behrens, M.; Gold, A.P.; Odel, J.; Olarte, M.R. Hypopigmented iris spot. An early sign of tuberous sclerosis. *Ophthalmology* **1982**, *89*, 1155–1159. [[CrossRef](#)]
37. Kim, Y.H.; Jo, D.S.; Park, N.Y.; Bae, J.E.; Kim, J.B.; Lee, H.J.; Kim, S.H.; Kim, S.H.; Lee, S.; Son, M.; et al. Inhibition of BRD4 Promotes Pexophagy by Increasing ROS and ATM Activation. *Cells* **2022**, *11*, 2839. [[CrossRef](#)] [[PubMed](#)]
38. Ghorpade, D.S.; Ozcan, L.; Zheng, Z.; Nicoloso, S.M.; Shen, Y.; Chen, E.; Bluher, M.; Czech, M.P.; Tabas, I. Hepatocyte-secreted DPP4 in obesity promotes adipose inflammation and insulin resistance. *Nature* **2018**, *555*, 673–677. [[CrossRef](#)]
39. Kong, L.; Deng, J.; Zhou, X.; Cai, B.; Zhang, B.; Chen, X.; Chen, Z.; Wang, W. Sitagliptin activates the p62-Keap1-Nrf2 signalling pathway to alleviate oxidative stress and excessive autophagy in severe acute pancreatitis-related acute lung injury. *Cell Death Dis.* **2021**, *12*, 928. [[CrossRef](#)]
40. Song, Y.; Yang, H.; Kim, J.; Lee, Y.; Kim, S.H.; Do, I.G.; Park, C.Y. Gemigliptin, a DPP4 inhibitor, ameliorates nonalcoholic steatohepatitis through AMP-activated protein kinase-independent and ULK1-mediated autophagy. *Mol. Metab.* **2023**, *78*, 101806. [[CrossRef](#)]
41. Arab, H.H.; Gad, A.M.; Reda, E.; Yahia, R.; Eid, A.H. Activation of autophagy by sitagliptin attenuates cadmium-induced testicular impairment in rats: Targeting AMPK/mTOR and Nrf2/HO-1 pathways. *Life Sci.* **2021**, *269*, 119031. [[CrossRef](#)]
42. Wesley, U.V.; Albino, A.P.; Tiwari, S.; Houghton, A.N. A role for dipeptidyl peptidase IV in suppressing the malignant phenotype of melanocytic cells. *J. Exp. Med.* **1999**, *190*, 311–322. [[CrossRef](#)]
43. Pethiyagoda, C.L.; Welch, D.R.; Fleming, T.P. Dipeptidyl peptidase IV (DPPIV) inhibits cellular invasion of melanoma cells. *Clin. Exp. Metastasis* **2000**, *18*, 391–400. [[CrossRef](#)]
44. Beckers, P.A.J.; Gielis, J.F.; Van Schil, P.E.; Adriaensen, D. Lung ischemia reperfusion injury: The therapeutic role of dipeptidyl peptidase 4 inhibition. *Ann. Transl. Med.* **2017**, *5*, 129. [[CrossRef](#)]
45. Sun, S.C. The non-canonical NF-kappaB pathway in immunity and inflammation. *Nat. Rev. Immunol.* **2017**, *17*, 545–558. [[CrossRef](#)] [[PubMed](#)]

46. Englaro, W.; Bahadoran, P.; Bertolotto, C.; Busca, R.; Derijard, B.; Livolsi, A.; Peyron, J.F.; Ortonne, J.P.; Ballotti, R. Tumor necrosis factor alpha-mediated inhibition of melanogenesis is dependent on nuclear factor kappa B activation. *Oncogene* **1999**, *18*, 1553–1559. [[CrossRef](#)]
47. Fu, C.; Chen, J.; Lu, J.; Yi, L.; Tong, X.; Kang, L.; Pei, S.; Ouyang, Y.; Jiang, L.; Ding, Y.; et al. Roles of inflammation factors in melanogenesis (Review). *Mol. Med. Rep.* **2020**, *21*, 1421–1430. [[CrossRef](#)]
48. Wang, X.; Ke, J.; Zhu, Y.J.; Cao, B.; Yin, R.L.; Wang, Y.; Wei, L.L.; Zhang, L.J.; Yang, L.Y.; Zhao, D. Dipeptidyl peptidase-4 (DPP4) inhibitor sitagliptin alleviates liver inflammation of diabetic mice by acting as a ROS scavenger and inhibiting the NFkappaB pathway. *Cell Death Discov.* **2021**, *7*, 236. [[CrossRef](#)]
49. Jeong, D.; Qomaladewi, N.P.; Lee, J.; Park, S.H.; Cho, J.Y. The Role of Autophagy in Skin Fibroblasts, Keratinocytes, Melanocytes, and Epidermal Stem Cells. *J. Investig. Dermatol.* **2020**, *140*, 1691–1697. [[CrossRef](#)]
50. Li, Y.F.; Ouyang, S.H.; Tu, L.F.; Wang, X.; Yuan, W.L.; Wang, G.E.; Wu, Y.P.; Duan, W.J.; Yu, H.M.; Fang, Z.Z.; et al. Caffeine Protects Skin from Oxidative Stress-Induced Senescence through the Activation of Autophagy. *Theranostics* **2018**, *8*, 5713–5730. [[CrossRef](#)]

Disclaimer/Publisher’s Note: The statements, opinions and data contained in all publications are solely those of the individual author(s) and contributor(s) and not of MDPI and/or the editor(s). MDPI and/or the editor(s) disclaim responsibility for any injury to people or property resulting from any ideas, methods, instructions or products referred to in the content.